ac band conductivity in compensated semiconductors with potential fluctuations

B. Pistoulet, F. M. Roche, and S. Abdalla
Laboratoire d'Automatique et de Microélectronique de Montpellier, Université des Sciences et Techniques du Languedoc, place Eugène Bataillon, F-34060 Montpellier Cédex, France
(Received 30 April 1984)

In compensated semiconductors, the occurrence of potential fluctuations which affect the local probability of ionization of deep levels cannot be ignored. These fluctuations strongly change the frequency and temperature dependence of the conductivity due to carriers in the bands. The expressions of ac and dc conductivity and of permittivity are derived in the case of a Gaussian distribution of fluctuations. It is shown that, starting from the densities and energies of impurities in the sample, the theory leads to a very accurate description of the observed conductivity in quite different cases: semi-insulating GaAs (our data), crystalline silicon (data of Pollak and Geballe). It is demonstrated that the carriers in the band are solely responsible for the observed phenomena, provided that potential fluctuations are taken into account. Band carrier conduction completely hides hopping conduction. Similar conclusions are obtained from the interpretation of data of the literature as well as our data, on amorphous semiconductors. It is inferred that the phenomena observed on a large variety of semiconductors merely reflect the same general effect of potential fluctuations on band carriers, rather than specific processes characteristic of the material.

I. INTRODUCTION

In the present paper, we analyze ac conductivity due to band carriers in compensated and semi-insulating semiconductors exhibiting potential fluctuations, in the crystalline or in the amorphous state. It has been recognized for a long time that, in compensated materials, potential fluctuations must result from the nonuniform distribution of impurities and the absence of screening by free carriers. Potential fluctuations were first considered by Shockley and Bardeen[1] and later by Keldysh and Proshko.[2] Schklowskii and Efros[3] analyzed the effect of the random potential due to impurities on the activation energies of dc impurity conductivity, in strongly compensated semiconductors. Redfield[4] proposed a band tail model for the study of dc transport properties in disordered semiconductors. Potential fluctuations have also been considered by Fritzsche[5] in the case of amorphous semiconductors. However, these papers did not end in an explicit formulation of transport coefficients in the presence of potential fluctuations. Expressions of dc transport coefficients in the presence of a Gaussian distribution of medium- or long-range potential fluctuations were derived by Pistoulet *et al.*[6] It has been shown by Girard[7] that the Fermi level, the dc conductivity activation energy, the lifetimes, and the photoconductivity are strongly dependent of both the magnitude of fluctuations and the degree of compensation of deep levels. Except in particular cases, dc transport properties of compensated semiconductors cannot be accounted for by reference to a hypothetical equivalent homogeneous material.

Extensive measurements of ac conductivity in crystalline, glassy, and amorphous semiconductors have been performed in many laboratories during the last decades. Since the famous paper of Pollak and Geballe[8] (hereafter known as PG) who attributed to a hopping process the $\sigma_{ac} \propto \omega^s$ law observed on the ac conductivity of silicon single crystals at low temperature, a large amount of literature was published on the subject. Surprisingly, little interest has been devoted to the contribution of band carriers located in potential wells to the ac conductivity of high-resistivity materials, and no formulation has been developed in order to take this effect into account until now.

In this paper, we propose a suitable model for quantitative evaluation of dc and ac conduction by band carriers, in high-resistivity semiconductors in which potential fluctuations play an essential part and cannot be ignored. It is shown that, in crystalline materials, the available data are completely explained by this process, and are not relevant to hopping. The same process is also significant in amorphous semiconductors, and likely overcomes other effects.

In Sec. II original expressions of ac and dc conductivities $\sigma_{ac}(\omega,T)$, $\sigma_{dc}(T)$ and ac permittivity $\epsilon_{ac}(\omega,T)$ are derived. The temperature and frequency dependences are drastically changed by the existence of potential fluctuations, as shown by numerical calculations; in particular, σ_{ac} due to band carriers starts from σ_{dc}, grows as ω^s in a fairly large range of frequency, then saturates as $\omega \rightarrow \infty$.

Section III deals with the distribution of carriers between impurities and bands in the presence of fluctuations. The nonuniform ionization of deep levels is taken into account in the derivation of carrier density.

In Sec. IV, we report conductivity data on semi-insulating GaAs single crystals versus temperature, between dc and 200 MHz. These data, which are not explained by existing models, confirm quite accurately the predictions of the theory. The combined effect of potential fluctuations and deep centers is clearly proved, and a self-consistent explanation based on the knowledge of deep levels density and energy is obtained.

In Sec. V, the data of Pollak and Geballe on Si single

crystals at low temperature are discussed, taking into account the role of band carriers provided by the impurities, in the presence of potential fluctuations. It is demonstrated that, in the whole temperature and frequency ranges considered by PG, the band carriers, which were disregarded by the authors, are entirely responsible for the observed behavior. The contribution of high-mobility band carriers is likely predominant and completely overcomes hopping conduction.

In Sec. VI, we analyze data on ac conductivities in amorphous silicon and germanium films in light of the above theory. It is shown that, in these materials too, band carriers in potential wells contribute significantly to ac and dc conductivities.

II. DERIVATION OF ac COMPLEX CONDUCTIVITY DUE TO BAND CARRIERS

We consider n-type compensated semiconductors in which the band carrier density is small compared to the total density of ionized impurities; therefore potential fluctuations due to the nonuniform distribution of impurities are not noticeably screened by free carriers. Moreover, it is assumed that, at temperatures of interest, the density of deep ionized centers remains small compared to the density of fully ionized shallow impurities which are thus mainly responsible for potential fluctuations. The spatial extent of the fluctuations is assumed larger than the carrier mean-free path and the Debye screening length.

According to the model of long-range potential fluctuations described in Ref. 6, the energy $E_c(\vec{r})$ of the conduction-band edge fluctuates in the sample according to a Gaussian distribution $P(E_c)$ reaching its maximum at E_{c0}, with a standard deviation $\Gamma/\sqrt{2}$. This distribution must be truncated at $E_{c0}\pm g\Gamma$, where g is a number ranging between 1 and 3 because unlikely deep wells (or hills) become screened, even by few carriers, when $\Gamma/kT \gg 1$. The possible temperature dependence of g is discussed in Sec. III. Moreover, the spatial probability of finding wells and hills is not necessarily the same, as illustrated in Fig. 1 in a particular case. Introducing the spatial probability α of wells, the total probability becomes $\alpha P(E_c)$ if $E_c < E_{c0}$, and $(1-\alpha)P(E_c)$ if $E_c > E_{c0}$. In order to simplify, α is assumed independent of the depth of the wells and characteristic of the specimen. Considering the reduced fluctuation amplitude

$$u = |E_c - E_{c0}|/\Gamma , \tag{1}$$

and the probability $P(u)=a\exp(-u^2)$, the normalization constant a is given by

$$\alpha\int_{-g}^{0} e^{-u^2}du + (1-\alpha)\int_{0}^{g} e^{-u^2}du = 1/a . \tag{2}$$

We shall neglect the small variation of the norm due to the truncation of the Gaussian function, and so $a \simeq 2/\sqrt{\pi}$. We write

$$n_{00} = N_c \exp[(E_F - E_{c0})/kT] , \tag{3}$$

and the carrier density in a well of depth u (with $u>0$) is $n_{00}\exp(u\Gamma/kT)$, and the density in a hill of the same height is $n_{00}\exp(-u\Gamma/kT)$. Therefore the average carrier density n_0 in the sample can be written as

$$n_0 = 2n_{00}\pi^{-1/2}\int_0^g [(\alpha\exp(u\Gamma/kT)+(1-\alpha)\exp(-u\Gamma/kT)]\exp(-u^2)du . \tag{4}$$

The conductivity of an inhomogeneous medium may be calculated by referring to a network of random valued conductances, as was shown by Kirkpatrick.[9] In particular, several models of random resistor networks were proposed for calculation of percolation thresholds and probabilities. However, this method is not very suitable for deriving an analytical expression of the conductivity and permittivity of the medium, which is our purpose in the present paper. In order to express the macroscopic ac complex conductivity of the sample, some general assumptions on the spatial arrangement of wells and hills must be introduced.

Let us consider that the conductivity of the sample as the sum of the conductivities of minute elements, each element consisting of a well and a hill of same height, and of relative length α and $(1-\alpha)$ in series (Fig. 1). The conductivity $\sigma_{ac}(u)$ and the permittivity $\epsilon_{ac}(u)$ of one element may be expressed as functions of the conductivity σ_0 in the hill and $\sigma_0+\sigma_l$ in the well

$$\sigma_{ac}(u) = \sigma_0 + \alpha\sigma_l \frac{\sigma_0[\sigma_0+\sigma_l(1-\alpha)]+\omega^2\epsilon_{sc}^2}{[\sigma_0+\sigma_l(1-\alpha)]^2+\omega^2\epsilon_{sc}^2} \tag{5}$$

$$\epsilon_{ac}(u) = \epsilon_{sc}\left[1+\frac{\alpha(1-\alpha)\sigma_l^2}{[\sigma_0+\sigma_l(1-\alpha)]^2+\omega^2\epsilon_{sc}^2}\right] , \tag{6}$$

where ϵ_{sc} is the lattice semiconductor permittivity and ω the angular frequency. Introducing the band carrier conductivity $\sigma_{00}=n_{00}q\mu_n$ at E_{c0}, the expressions of σ_0 and $\sigma_0+\sigma_l$ are

$$\sigma_0 = \sigma_{00}\exp(-u\Gamma/kT) ,$$

$$\sigma_0+\sigma_l = \sigma_{00}\exp(u\Gamma/kT) .$$

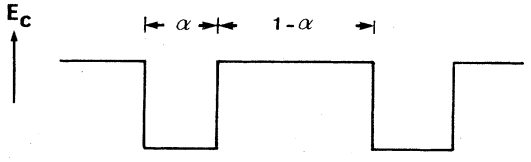

FIG. 1. Sketch of wells and hills of same magnitude in series.

The average complex conductivity $\sigma_{ac}+i\omega\epsilon_{ac}$ of the sample is the sum of the contributions of the different elements, weighted by their probability:

$$\sigma_{ac}+i\omega\epsilon_{ac}=\int[\sigma_{ac}(u)+i\omega\epsilon_{ac}(u)]P(u)du\ . \tag{7}$$

We write

$$x=\alpha\exp(-u\Gamma/kT)+(1-\alpha)\exp(u\Gamma/kT) \tag{8}$$

and

$$\tau_{00}=\epsilon_{sc}/\sigma_{00}\ , \tag{9}$$

then

$$\sigma_{ac}/\sigma_{00}=\frac{2}{\pi^{1/2}}\int_0^g\left\{1+\alpha[\exp(2u\Gamma/kT)-1]\frac{x\exp(-u\Gamma/kT)+\omega^2\tau_{00}^2}{x^2+\omega^2\tau_{00}^2}\right\}\exp(-u^2-u\Gamma/kT)du\ , \tag{10}$$

$$\epsilon_{ac}/\epsilon_{sc}=1+\frac{8\alpha(1-\alpha)}{\pi^{1/2}}\int_0^g\frac{\sinh^2u\Gamma/kT}{x^2+\omega^2\tau_{00}^2}\exp(-u^2)du\ . \tag{11}$$

These expressions are valid in the whole range of frequency including dc and high-frequency limits. The dc conductivity and permittivity are obtained from Eqs. (10) and (11) when $\omega\rightarrow 0$:

$$\sigma_{dc}/\sigma_{00}=2\pi^{-1/2}\int_0^g x^{-1}\exp(-u^{2})du\ , \tag{12}$$

$$\epsilon_{dc}/\epsilon_{sc}=1+8\pi^{-1/2}\alpha(1-\alpha)\int_0^g x^{-2}\sinh^2(u\Gamma/kT)\exp(-u^2)du\ . \tag{13}$$

As the frequency tends to infinity, the conductivity tends towards the high-frequency limit $\sigma_\infty=n_0q\mu_n$ given by

$$\sigma_\infty/\sigma_{00}=2\pi^{-1/2}\int_0^g[\alpha\exp(u\Gamma/kT)+(1-\alpha)\exp(-u\Gamma/kT)]\exp(-u^2)du \tag{14}$$

and ϵ_{ac} tends to ϵ_{sc}. Equations (10), (12), and (14) give σ_{ac} and σ_{dc} when Γ, g, α, and σ_∞ are known. Results of numerical calculations are discussed in following sections. They indicate that, as ω increases, σ_{ac} starting from σ_{dc} increases as ω^s in rather wide ranges of frequency and temperature, then, tends towards a high-frequency limit σ_∞. The exponent s remains smaller than unity, and its variations are plotted, in Fig. 2, versus Γ/kT for $\alpha=0.23$ in two cases: The full line corresponds to $g=2.5$, the dotted line to $g=bT$ (as explained later) with $b=6.7\times10^{-3}$. This shows that the occurrence of a $\sigma_{ac}\propto\omega^s$ law may result from the influence of potential fluctuations on band conduction, and is not necessarily associated with a hopping process. It is the same for the $T^{-1/4}$ dependence of σ_{dc}: when σ_∞ is independent of temperature, σ_{dc} calculated from Eq. (12) may follow this law in significant temperature ranges. In order to decide which process is involved, the first step consists of calculating the total carrier density n_0 in the band, starting from the knowledge of the density of impurities and their ionization energy. It is then possible to compare the conductivity $\sigma_{ac}(\omega,T)$ due to band carriers to the measured one, and to decide if another process is predominant or not.

III. DISTRIBUTION OF CARRIERS BETWEEN IMPURITIES AND BANDS

As has been pointed out in Ref. 7, local neutrality does not exist in the presence of potential fluctuations. If the semiconductor is macroscopically homogeneous, an average neutrality equation may be written by averaging the carrier density and the impurity density over the sample. These average densities are physically observable quantities, whereas local densities are not, because any measur-

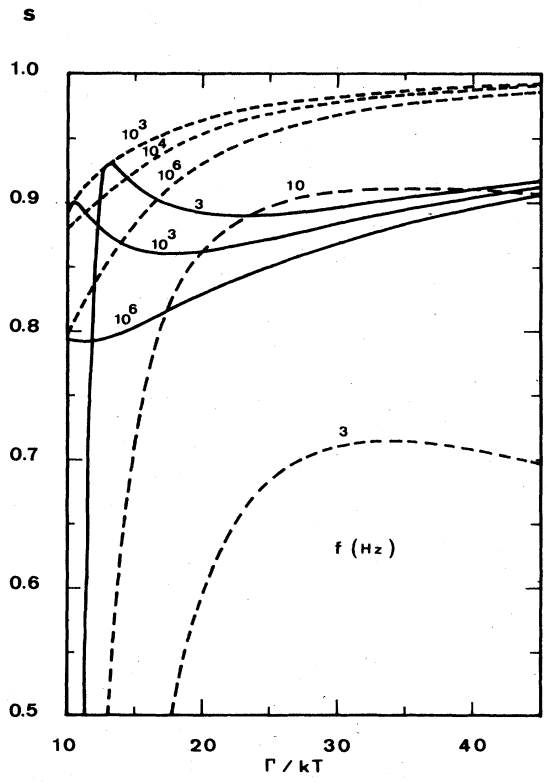

FIG. 2. Exponent s of the $\sigma_{ac}\propto\omega^s$ law versus Γ/kT with frequency as parameter, for band conduction in presence of potential fluctuations ($\alpha=0.23$, solid line $g=2.5$, dotted line $g=6.7\times10^{-3}T$).

able sample contains a large number of elements. The local ionization probability $N_{dd}^{+}(\vec{r})/N_{dd}$ of deep donors, or $N_{da}^{-}(\vec{r})/N_{da}$ of deep acceptors, depends on the local potential $E_c(\vec{r})$, so that it is strongly affected by the amplitude of potential fluctuations:

$$\frac{N_{dd}^{+}(\vec{r})}{N_{dd}}=\left[1+g_{dd}\exp\left[\frac{E_F-E_c(\vec{r})+E_{dd}}{kT}\right]\right]^{-1}, \tag{15}$$

$$\frac{N_{ad}^{-}(\vec{r})}{N_{ad}}=\left[1+g_{da}^{-1}\exp\left[\frac{E_c(\vec{r})-E_G+E_{da}-E_F}{kT}\right]\right]^{-1}, \tag{16}$$

where g_{dd} (g_{da}) is the ratio of the degeneracy of the occupied and unoccupied donor (acceptor) state, and E_{dd} (E_{da}) is the ionization energy of the donor (acceptor) in the conduction (valence) band. We shall restrict our purpose to the consideration of one species of deep donor, and one of deep acceptor; moreover shallow donors and acceptors of respective densities N_{sd}, N_{sa} are assumed to remain fully ionized at every point of the material in the whole temperature range of experiments. Using Eq. (4), and writing

$$n_{00}/n_0=m\ , \tag{17}$$

the average neutrality equation is

$$n_0-p_0=N_{sd}-N_{sa}+N_{dd}^{+}-N_{da}^{-}\ , \tag{18}$$

where

$$N_{dd}^{+}=\frac{2(1-\alpha)}{\pi^{1/2}}\int_0^g N_{dd}\left[1+g_{dd}\frac{mn_0}{N_c}\exp[(E_{dd}-u\Gamma/kT]\right]^{-1}\exp(-u^2)du\ ,$$

$$+\frac{2\alpha}{\pi^{1/2}}\int_0^g N_{dd}\left[[1+g_{dd}\frac{mn_0}{N_c}\exp[(E_{dd}+u\Gamma)/kT]\right]^{-1}\exp(-u^2)du\ , \tag{19}$$

$$N_{da}^{-}=\frac{2(1-\alpha)}{\pi^{1/2}}\int_0^g N_{da}\left[1+\frac{N_c}{g_{da}mn_0}\exp[(E_{da}-E_G+u\Gamma)/kT]\right]^{-1}\exp(-u^2)du$$

$$+\frac{2\alpha}{\pi^{1/2}}\int_0^g N_{da}\left[1+\frac{N_c}{g_{da}mn_0}\exp[(E_{da}-E_G-u\Gamma)/kT]\right]^{-1}\exp(-u^2)du\ . \tag{20}$$

The densities N_{dd},N_{da} appearing in the integrals are unknown functions of u. It is assumed that the potential fluctuations result mainly from the nonuniform distribution of shallow impurities, so that N_{dd} and N_{da} do not depend very strongly on u, and they may be replaced by constants. Then the integrals in Eqs. (19) and (20) may be computed, and the average carrier density n_0 is given by Eq. (18). In this equation p_0, if not negligible, must be replaced by

$$p_0=2\pi^{-1/2}(n_i^2/mn_0)\int_0^g[\alpha\exp(-u\Gamma/kT)+(1-\alpha)\exp(u\Gamma/kT)]\exp(-u^2)du\ . \tag{21}$$

Before comparing with experiment, let us examine the temperature dependence of the maximum depth of the wells. At very low temperature, $g\Gamma/kT$ tends to become very large, so the n_0 carriers per unit volume accumulate in the few deepest wells; as a consequence, the deepest wells are partly screened even if n_0 is small. On the other hand, the Fermi level must be very close to the bottom of these wells in order to account for the population of the band; so the Fermi level is pinned at some kT of the bottom of the deepest wells. The depth $g\Gamma$ must adjust to a value such that n_0 calculated by Eq. (4), with $E_{c0}-E_F\simeq g\Gamma$ in Eq. (3), is equal to the net density $N_{sd}-N_{sa}$ of exhausted shallow levels. In high-resistivity materials, such as those considered below, $g\Gamma/kT$ at low temperature is of the order of 20 or more, so that n_0 in Eq. (4) is approximately a function of $g\Gamma/kT$ only. Thus, as long as n_0 remains constant g is nearly proportional to T. At very low temperature $\sigma_{dc}/\sigma_\infty$ is also nearly a function of $g\Gamma/kT$ only; therefore, σ_{dc} must be approximately independent of T. The increase of g with temperature leads to more and more improbable deepest wells with a reduced size. The maximum depth of wells is necessarily limited above a given temperature, depending on the sample, to some value $g_m\Gamma$, due to the increase of the Debye screening length. Above this temperature, the Fermi level moves away from the bottom of the wells and g is expected to remain constant until ionization of deep levels starts. The ionization of deep donors occurs in the highest potential energy hills of height $g_m\Gamma$, when that of deep acceptors occurs in the deepest wells of depth $g_m\Gamma$. Thus fixed positive (or negative) charges appear at the places where the electrostatic potential is minimum (or maximum), and this tends to locally neutralize the shallow impurity charges responsible for large fluctuations of low probability. This effect clearly results in a reduction of g as T increases; this decrease must be limited by the increase of the probability of wells of reduced depth. It must be noted that, as long as the density of ionized deep impurities remains small, compared to the total density of shallow impurities, no significant variation of Γ may happen so that, in the cases examined below, Γ is considered as a constant in the whole range of temperature in which measurements are made.

IV. SEMI-INSULATING GaAs

In this section, we report complex permittivity measurements between 0.1 Hz and 200 MHz, performed on a

Cr-doped GaAs single crystal provided by LEP. According to the manufacturer's specifications, the Cr content is between 1 and 3×10^{16} cm^{-3}. The sample has been annealed at 850 °C for 15 min. Measurements are made on disks 0.3 mm thick and of 4 mm in diameter, with Au-Ge ohmic contacts on both sides. Complex permittivity measurements are performed with a frequency response analyzer from 0.1 Hz to 1 MHz. Between 1 and 200 MHz, the sample is inserted in a coaxial line, and the transmission and reflection coefficients are determined by a standard reflectometry method. The line is arranged in a cryostat enabling us to vary the temperature of the sample between 240 and 410 K. Some complementary room-temperature measurements were made at 10 GHz in a high-Q cavity on samples without contacts.

Full points on Figs. 3 and 4 show experimental values of σ_{dc}, $\sigma_{ac}(\omega)$, and $\epsilon_{ac}(\omega)$, with T as a parameter. The general shape of the curves reflects the expected variations of conductivity due to band carriers, as they are described by Eqs. (10)—(14). However, small bumps on the σ_{ac} curves, associated with large increases of ϵ_{ac} above ϵ_{sc} are relevant to the charge and discharge of deep centers with finite-time constant. This effect, which was extensively studied in the case of p-n junctions and Schottky barriers,[10,11] is particularly significant in semi-insulating semiconductors, owing to the large number of barriers between domains, in which deep levels are able to cross the Fermi level. Thus, before analyzing the frequency and temperature dependence of complex conductivity due to band carriers, the first step consists in properly evaluating the contribution of charging and discharging these centers. Using the results of Zohta,[11] the contributions of center i to σ_{ac} and ϵ_{ac} are

$$(\sigma_{ac})_i=\frac{\omega^2\tau_i}{1+\omega^2\tau_i^2}(\epsilon_{LF}-\epsilon_{HF})_i\ , \tag{22}$$

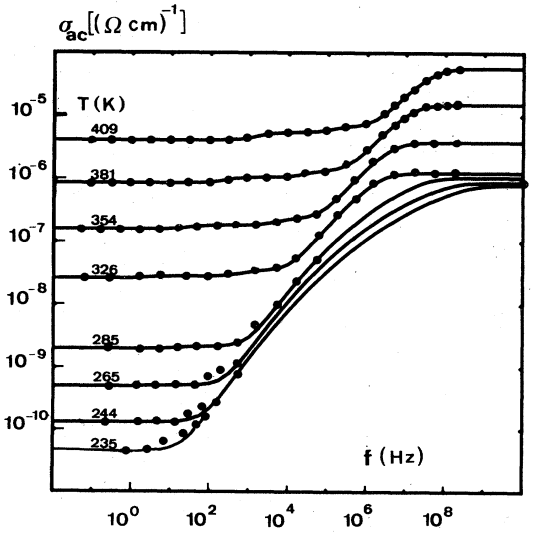

FIG. 3. (●) Experimental $\sigma_{ac}(\omega,T)$ data on semi-insulating GaAs sample. Solid lines: σ_{ac} calculated by Eqs. (10) and (25).

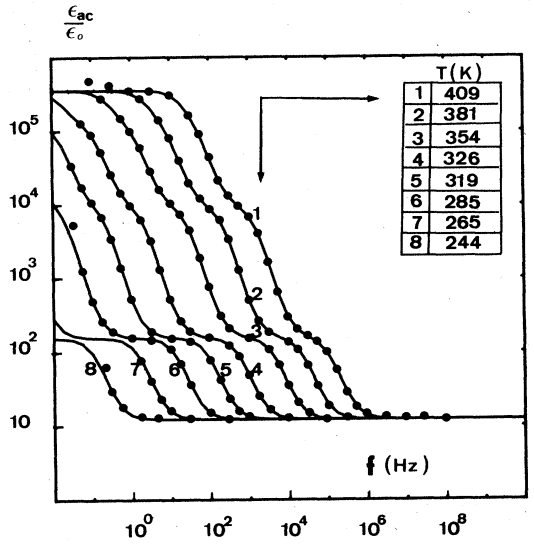

FIG. 4. (●) Experimental $\epsilon_{ac}(\omega,T)$ data on semi-insulating GaAs sample. Solid lines: ϵ_{ac} calculated by Eqs. (11) and (26).

$$(\epsilon_{ac}-\epsilon_{HF})_i=\frac{(\epsilon_{LF}-\epsilon_{HF})_i}{1+\omega^2\tau_i^2}\ , \tag{23}$$

where $(\epsilon_{LH}-\epsilon_{HF})_i$ is the dielectric permittivity variation when ω goes from values much smaller to values much larger than $1/\tau_i$. The values of $(\epsilon_{LF}-\epsilon_{HF})_i$ are determined from ϵ_{ac} data (Fig. 4). The value of $1/\tau_i$ is the angular frequency at which the experimental curve $(\sigma_{ac})_i/\omega$ plotted versus ω, at constant temperature, goes through a maximum. As τ_i is proportional to the reverse of the electron emission rate of the center, it is characterized by an activation energy E_i and a high-temperature limit τ_{i0} which are determined by extrapolating the experimental data (Fig. 5):

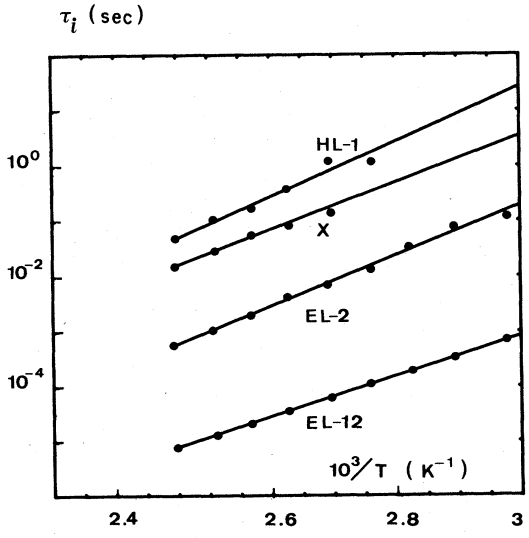

FIG. 5. τ_i versus $10^3/T$ in semi-insulating GaAs sample.

$$\tau_i = \tau_{i0}\exp(E_i/kT) \ . \tag{24}$$

Four deep levels are noticed on the curves, and their ionization energy is calculated from τ_i versus T^{-1} plots by Eq. (24). Two of these levels are identified as EL2 and HL1, a third one possibly as EL12. The last one appearing at low frequency and high temperature is named X. In the numerical calculation of permittivity we take into account the known temperature dependence of EL2 and HL1:[12]

$$E_i(\text{EL2}) = 0.752 - 2.37\times10^{-4}T(\text{K}) \text{ eV} \ ,$$

$$E_i(\text{HL1}) = E_G - \{0.81 - 3\times10^{-4}[T(\text{K})]^2/[T(\text{K}) + 204 \text{ (K)}] + kT\ln 0.93\} \ .$$

In a similar way we assume for EL12

$$E_i(\text{EL12}) = 0.67 - 3.2\times10^{-4}T(\text{K}) \text{ eV} \ .$$

In the absence of other information, the energy of the last level is assumed equal to

$$E_i(X) = 0.78 - 2.7\times10^{-4}T(\text{K}) \text{ eV} \ .$$

The values of $(\epsilon_{\text{LF}} - \epsilon_{\text{HF}})_i, \tau_{i_0}$ are listed in Table I. The total contribution of charging and discharging the centers at a given temperature is the sum of the individual contributions:

$$(\sigma_{\text{ac}})_{\text{center}} = \sum_i (\sigma_{\text{ac}})_i \ , \tag{25}$$

$$(\epsilon_{\text{ac}} - \epsilon_{\text{HF}})_{\text{center}} = \sum_i (\epsilon_{\text{ac}} - \epsilon_{\text{HF}})_i \ . \tag{26}$$

The total calculated permittivity $\epsilon_{\text{sc}} + (\epsilon_{\text{ac}} - \epsilon_{\text{HF}})_{\text{center}}$ is shown in Fig. 4. Agreement with the data is good at all temperatures and frequencies.

Let us now come back to the effect of band carriers. It is obvious in Fig. 3 that, at high frequency, σ_{ac} tends to a limit which is reached around 100 MHz. This conclusion has been confirmed by 10-GHz room-temperature measurements. From the experimental values of σ_∞ and σ_{dc} plotted versus $1/T$ in Fig. 6 it is possible to compute Γ using Eqs. (12) and (14), for given values of the parameters α and g. Below 280 K, no appreciable ionization of deep centers is observed, so g must stay roughly constant. Starting from an arbitrary value of α, one tries to find suitable Γ and g values, by successive approximations. The cycle is repeated until a good fit of experimental data is reached. Figure 3 shows the results obtained with $\alpha = 0.47$, $\Gamma = 120$ meV, $g(T)$ given by Fig. 7; this variation of g is quite in agreement with the expected one at low temperature, as well as at high temperature where ionization of deep levels occurs. Moreover $n_0(T)$ may be calculated by Eq. (18) and the corresponding values of $\sigma_\infty(T)$ compared to the experimental ones. At low temperature, $(\sigma_\infty)_{\text{exp}} = 8\times10^{-7}$ $(\Omega\,\text{cm})^{-1}$ so with $\mu_n = 3200$ $\text{cm}^2/\text{V s}$, we find $N_{\text{sd}} - N_{\text{sa}} = 1.56\times10^9$ cm^{-3}. Taking $N_{\text{da}}(\text{HL1}) = 1.44\times10^{16}$ cm^{-3} (in the range of manufacturer specification) and $N_{\text{dd}}(\text{EL2}) = 5\times10^{16}$ cm^{-3} which is of the usual order of magnitude, we obtain the fit shown in Fig. 6. The Fermi-level position at $T = 381$ K is shown in Fig. 8 where energy is in ordinate, and probability $P(E_c)$ in abscissa. The local energy of deep levels is represented by curves shifted by a quantity E_i from E_c. The average degree of ionization of a level can thus be deduced from the abscissa at which the corresponding curve intersects the Fermi level. It is clear that, due to the existence of potential fluctuations, many deep levels cross the Fermi level, and this explains the magnitude of previously mentioned effects of charging and discharging these centers. The position of the Fermi level as T varies is compared to that of the bottom of deepest wells in Fig. 9. In summary, a complete self-consistent explanation of the experimental data is obtained from the knowledge of the densities and ionization energies of impurities, and of the magnitude of potential fluctuations, leaving no doubt on the actual conduction process. On the contrary, the data may not be explained by band conduction when ignoring fluctuations, and hopping theories are unable to predict accurately the variations of σ_{dc} and σ_{ac} in the large frequency and temperature ranges covered by experiment.

TABLE I. Values of $(\epsilon_{\text{LF}} - \epsilon_{\text{HF}})_i$, and τ_{i0} corresponding to the four observed deep levels.

Level	$(\epsilon_{\text{LF}} - \epsilon_{\text{HF}})_i/\epsilon_0$	τ_{i0} (s)
EL2	$(9.25-1)\times10^3$	5×10^{-12}
HL1	$(3.4-0.62)\times10^4$	8.6×10^{-13}
EL12	$(1.2-0.25)\times10^2$	1.9×10^{-12}
X	$(2-0.07)\times10^4$	8.7×10^{-11}

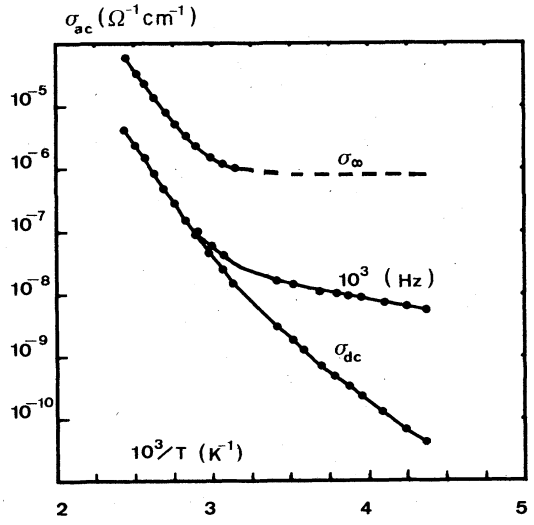

FIG. 6. σ_{dc}, σ_∞ versus $10^3/T$ in semi-insulating GaAs sample.

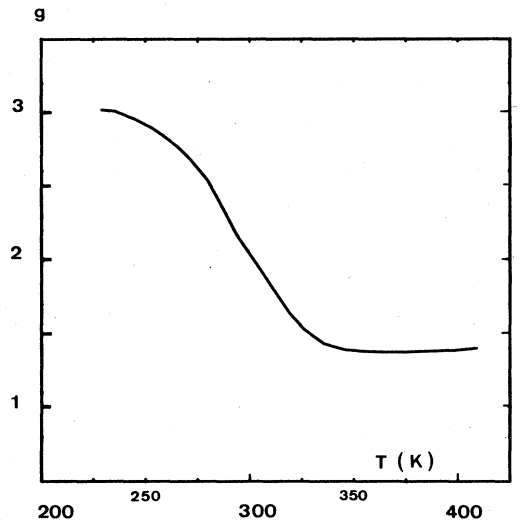

FIG. 7. $g(T)$ in semi-insulating GaAs sample.

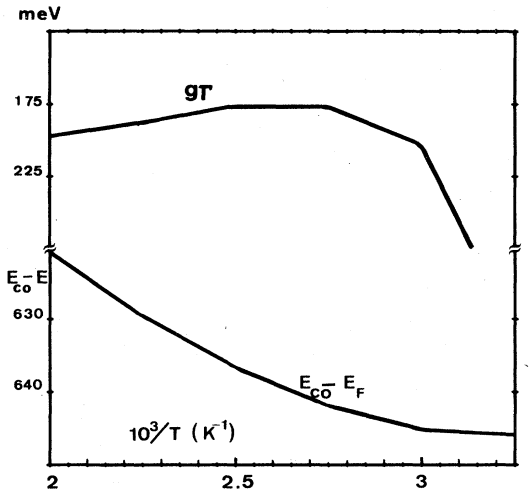

FIG. 9. Fermi level, and bottom of deepest wells, versus T in semi-insulating GaAs sample.

V. INTERPRETATION OF DATA OF POLLAK AND GEBALLE

Pollak and Geballe[8] reported experimental data on partially compensated Si single crystals at low temperature, and analyzed these results on the basis of a hopping theory. A limited set of frequencies was covered by measurements: 0, 10^2, 10^3, 10^4, and 10^5 Hz, and attention was mainly devoted to the $\sigma_{ac} \propto \omega^s$ law, which was observed between 10^2 and 10^5 Hz, with $s \simeq 0.8$. In the interpretation of data, there has been no attempt to take into account the contribution of band carriers, nor the influence of potential fluctuations. In this section, we shall analyze PG data in the light of our theory, particularly those concerning samples numbers 13 and 8 for which $\sigma_{ac}(T)$ characteristics between dc and 10^5 Hz are given by the authors.

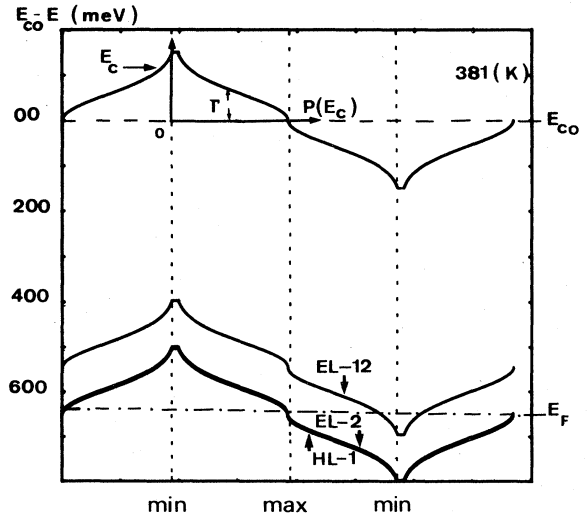

FIG. 8. Respective locations of Fermi level, and deep levels, in semi-insulating GaAs sample.

A. Sample number 13

The characteristics of the sample are N_a(boron) $=0.8\times10^{15}$ cm^{-3} and N_d(phosphorus) $=2.7\times10^{17}$ cm^{-3}. The experimental dc and ac conductivities (Fig. 5 of the original paper of PG) are reproduced in Fig. 10. In the

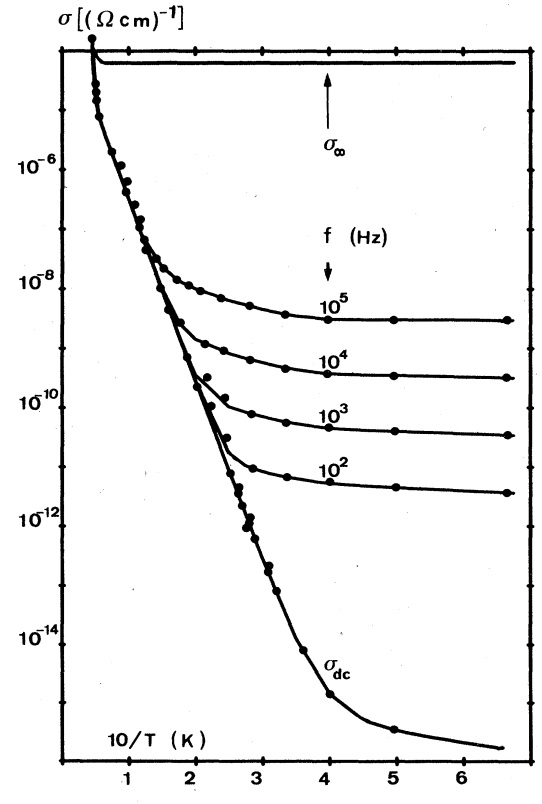

FIG. 10. (●) Experimental σ_{ac},σ_{dc} data of Pollak and Geballe on c-Si (sample number 13). Solid lines: Conductivities calculated according to Eqs. (10) and (12).

case of a partly compensated donor level, the neutrality equation in an n-type material is

$$n_0 = N_d^+ - N_a \ . \tag{27}$$

At low temperature, when $N_c \exp(-E_d/kT) \ll g_d N_a$, the solution of this equation may be approximated, neglecting potential fluctuations, by the classical expression

$$n_0 \simeq N_c (N_d - N_a)(g_d N_a)^{-1} \exp\left[-\frac{E_d}{kT}\right] , \tag{28}$$

where E_d is the ionization energy of the donors. In the case of phosphorus $E_d = 0.045$ eV, so with the values of N_a, N_d given by PG this leads to $n_0 \simeq 1.7 \times 10^8$ cm^{-3} at 20 K; this value is far too small to account for the experimental dc conductivity of 10^{-5} $(\Omega\,\text{cm})^{-1}$ at this temperature. The discrepancy is still getting worse as T decreases. This is possibly why the authors did not consider the conductivity due to electrons in the conduction band. But a careful examination of the experimental $\sigma_{dc}(T)$ curve reveals a sharp change of slope at about $T_i = 20.65$ K, near the upper left corner of the figure. This kink is very likely due to the ionization of a donor which, according to the doping of the sample, may only be phosphorus. Therefore, below T_i, band conduction electrons are not provided by phosphorus but by an unspecified shallow donor; this donor is possibly nitrogen whose maximum solubility in silicon is 4.5×10^{15} cm^{-3} (Ref. 13) and ionization energy $E_{sd} = 0.017$ eV, or a center of lower binding energy. This shallow donor, of density N_{sd} is exhausted and partly compensated by boron of density N_{sa}, with $N_{sa}/N_{sd} < 1$, and the phosphorus level is uncompensated. With $n_s = N_{sd} - N_{sa}$, the neutrality equation becomes

$$n_0 = n_s + N_d^+ \ . \tag{29}$$

The low-temperature density n_s is much smaller than N_a, as calculations will show. Then, near T_i, $N_d^+/N_d \ll 1$, the Fermi level is well above the donor level, so $N_c \exp(-E_d/kT) \ll n_s$. On the other hand, due to the fact that $n_s \ll N_d$,

$$N_c \exp(-E_d/kT) \gg g_d n_s^2/4(N_d + n_s)$$

and, as is well known, the solution of Eq. (29) then reduces to

$$n_0 \simeq [N_c(N_d + n_s)/g_d]^{1/2} \exp(-E_d/2kT) \ . \tag{30}$$

In writing that T_i is the temperature at which $N_d^+(T_i) = n_s$ we obtain

$$n_s = [N_c(N_d + n_s)/2g_d]^{1/2} \exp(-E_d/2kT_i) \ . \tag{31}$$

In the case of phosphorus, $E_d = 45$ meV, and this equation leads to $n_s = 5.4 \times 10^{11}$ cm^{-3}. As the experimental dc conductivity $\sigma_{dc}(T_i) = 1.07 \times 10^{-5}$ $(\Omega\,\text{cm})^{-1}$, the mobility would be roughly equal to 60 cm^2/V s.

We now consider the effect of potential fluctuations, and use the values of α, Γ, g found below by fitting the data. At temperatures lower than T_i, $\sigma_\infty = n_s q \mu_n$ remains constant, if we neglect the temperature dependence of mobility, and equal to 6.5×10^{-5} $(\Omega\,\text{cm})^{-1}$. On the other hand, $N_d^+(T_i)$ must be calculated by Eq. (19) in place of Eq. (31), so $n_s = 2.28 \times 10^{12}$ cm^{-3}, leading to a mobility $\mu_n = 178$ cm^2/V s, which is of the expected order of magnitude for this doping.

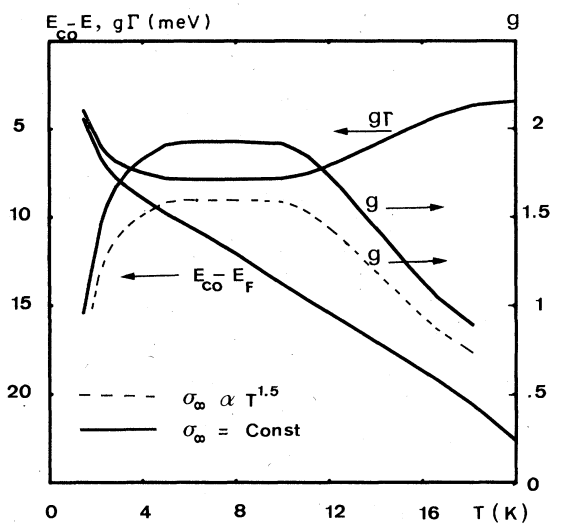

FIG. 11. $g(T)$, $g\Gamma$, $E_{c0} - E_F$ in c-Si sample number 13 (of Pollak and Geballe).

Above T_i, $\Gamma/kT < 2.5$, so potential fluctuations have minor consequences. On the contrary, at low temperature, i.e., in nearly all the range of PG measurements, $g\Gamma/kT$ is large, of the order of 29.6 at 2.5 K. In this range, $\sigma_\infty \gg \sigma_{dc}$, and potential fluctuations drastically change dc and ac conductivities. This is demonstrated by fitting the experimental conductivity data by means of Eqs. (10), (12), and (14). We first neglect the temperature dependence of mobility so, at low temperature $\sigma_\infty = 6.5 \times 10^{-5}$ $(\Omega\,\text{cm})^{-1}$. Again the search for the right values of α, Γ, $g(T)$ is done by successive approximations, starting from given trial values of α and Γ, and trying to fit the $\sigma_\infty/\sigma_{dc}$ and σ_{ac}/σ_{dc} variations. The cycle is repeated by adjusting the parameters until a good agreement with the experimental data of PG is reached. Below 2 K the σ_{dc} curve has been extrapolated. The best fit shown in Fig. 10 is obtained with $\alpha = 0.12$, $\Gamma = 4.06$ meV, and $g(T)$ as given by Fig. 11. As expected, $g(T)$ is proportional to T at low temperature, and tends to a limit equal to 1.9 for $5\ \text{K} \le T \le T_i$. If we take into account a temperature dependence $\mu_n \propto T^{3/2}$ of the mobility due to impurity scattering, the same fit is obtained by slightly modifying $g(T)$ (Fig. 11) and keeping the same α and Γ. In any case, a striking agreement between computed and experimental data is obtained in the whole temperature and frequency ranges. This fact leaves little doubt on the origin of observed phenomena.

B. Sample number 8

The characteristics given for this sample are N_a small; N_d (phosphorus) $= 1.5 \times 10^{16}$ cm^{-3}. PG data are reproduced in Fig. 12. The temperature range in which σ_{dc}

data are available extends only from 10 to 20 K. The plot of σ_{dc} versus $10/T$ shows an increase of activation energy at 12.5 K. This is likely the temperature T_i above which electrons are mainly supplied by ionization of phosphorus donors. Below T_i, electrons come from exhausted shallow levels, as in sample number 13, and consequently the phosphorus centers are uncompensated. If we first neglect the effect of potential fluctuations, the density of ionized P centers calculated by Eq. (31) is equal to $N_d^+(T_i)=2.5\times10^7$ cm^{-3} [whereas it would be negligible if P centers were compensated, according to Eq. (28)]. As $\sigma_{dc}(T_i)=1.62\times10^{-12}$ $(\Omega\,\text{cm})^{-1}$, this leads to a far too low mobility $\sigma_{dc}/q(n_s+N_d^+)\simeq0.4$ cm^2/V s, in a crystal where the total doping is of the order of 10^{16} cm^{-3}. Let us now consider the existence of potential fluctuations. Experimental data may be accurately fitted (Fig. 12) by choosing $\alpha=0.10$, $\Gamma=7.85$ meV, and $g(T)$ given by Fig. 13. With these characteristics of potential fluctuations, $n_s=N_d^+(T_i)$ obtained by Eq. (19) is equal to 1.130×10^8 cm^{-3}; $\sigma(T_i)/\sigma_{dc}(T_i)=6\times10^3$ therefore, $\sigma_\infty(T_i)=1.18\times10^{-8}$ $(\Omega\,\text{cm})^{-1}$. This gives $\mu_n=\sigma_\infty(T_i)/2qN_d^+(T_i)=106$ cm^2/V s which is of the right order of magnitude. It should be noticed that the only adjusted parameters concern the amplitude of potential fluctuations; the calculation of total carrier density is only based on impurity density and energy.

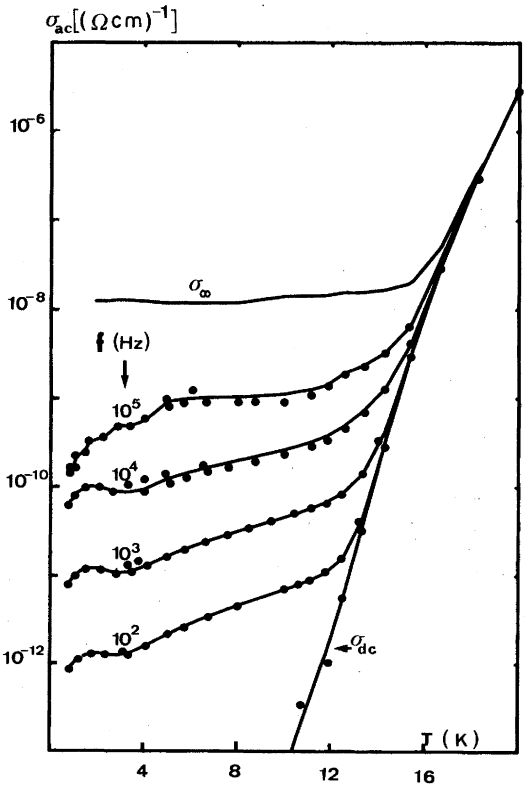

FIG. 12. (●) Experimental σ_{ac},σ_{dc} data of Pollak and Geballe on c-Si (sample number 8). Solid lines: Conductivities calculated according to Eqs. (10) and (12).

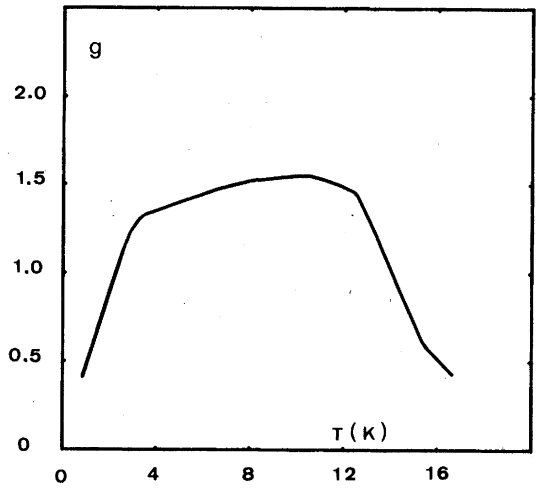

FIG. 13. $g(T)$ in c-Si sample number 8 of Pollak and Geballe.

In conclusion, in both samples, numbers 13 and 8 of PG, there is a non-negligible electron density in the conduction band; this is proved by calculating $N_d^+(T_i)$, and this corresponds to a quite normal value of mobility. Band electrons are entirely responsible for the observed conductivity data which reflect only the influence of potential fluctuations on these carriers. Hopping conductivity is probably orders of magnitude lower, and this is not very surprising if one considers the high mobility of carriers in the band. Therefore the PG data are similar to our data on semi-insulating GaAs and does not support a hopping mechanism.

VI. AMORPHOUS SEMICONDUCTORS

It is well known that some amorphous semiconductors are generally compensated, owing to their density of donor and acceptor states in the gap. On the other hand, it is now recognized that, in good quality materials, electrical conduction by carriers above the mobility edge is significant. Thus, in amorphous semiconductors, the presence of band carriers and the existence of potential fluctuations may contribute significantly to dc and ac conduction. In the following, this contribution will be evaluated using Eqs. (10)—(14). Contrary to the case of crystalline materials, available experimental data are often incomplete. The dc conductivity versus temperature and/or the high-frequency limit $\sigma_\infty(T)$ are generally unknown. On the other hand, little or uncertain information is available on the density of states in the gap. Therefore, some assumptions are needed in order to fit the data, but it is shown below how it is possible to greatly reduce the degree of uncertainty by considering various pieces of information such as location of the Fermi level, dependence of g versus T, and ionization of deep levels.

A. Data of Abkowitz *et al.* (Ref. 14) on glow discharge *a*-Si

The main features which are observed on the reported $\sigma_{ac}(\omega,T)$ curves (Fig. 14) are (i) the value of the exponent s which is nearly equal to unity, but slightly smaller, (ii) the spacing of isotherms, (iii) the existence of a deep center whose charge and discharge produces a large hump in the low-frequency range at high temperature, (iv) no indications on $\sigma_{dc}(T)$ nor $\sigma_\infty(T)$.

We first observe that low-temperature $\sigma_{ac}(\omega)$ curves are very similar to those found by Pollak and Geballe in *c*-Si. In order to evaluate the contribution of band carriers, we use Eqs. (10)—(14) for calculating $\sigma_{ac}(\omega,T)$, for various values of α, σ_∞, Γ, and g. At low temperature σ_∞ is considered as due to exhaustion of shallow levels. The choice of suitable value of σ_∞ is made by fitting σ_{ac} at high frequency, in the whole temperature range; this fit may only be obtained in a limited range of σ_∞ values, of the order of one decade. Besides, σ_∞ must lead to a value of band-carrier mobility of a reasonable order of magnitude. By successive approximations, the most suitable σ_∞ is found equal to 10^{-3} $(\Omega\,\mathrm{cm})^{-1}$, with $\alpha=0.23$. Then, at each temperature σ_{ac} is calculated by Eq. (10), compared to experimental data; Γ and g are varied until an agreement is reached. We thus obtain couples of Γ and g values; in order to find the right couple, g is plotted versus Γ with ω as a parameter. It is found that all the curves intersect at the same point which sets the values of Γ and $g(T)$. As T is varied, a unique solution is found for Γ which remains constant and equal to 320 meV, while g varies linearly with T as expected. Up to 240 K the Fermi level at low temperature must be about kT below the bottom of the deepest wells as previously explained; thus, considering an equivalent density of states N_c in the conduction band close to that of crystalline silicon, $E_{c0}-E_F$ is calculated by the equation

$$E_{c0}-E_F=kT\ln(q\mu_n N_c/m\sigma_\infty)\,, \tag{32}$$

where μ_n is the mobility, and $m=\sigma_{00}/\sigma_\infty$ is given by Eq. (14). In the absence of mobility data and of σ_∞ or σ_{dc} data, some assumption must be made. Mobility values of the order of 0.1 $\mathrm{cm^2/V\,s}$ have been reported, so we assume $\mu_n=0.3$ $\mathrm{cm^2/V\,s}$ at all temperatures, in order that E_F be located at kT below the bottom of deepest wells at low temperatures. However we must notice that a higher value of mobility could be chosen. If σ_∞ is considered as temperature independent, the Fermi level crosses the bottom of the wells around 280 K and goes slightly above $E_{c0}-g\Gamma$ at 340 K. However, the large hump observed in $\sigma_{ac}(\omega)$ curves at low frequency and high temperature is relevant from the charge and discharge of a deep level whose characteristics, obtained by fitting the data using Eq. (22), are

$$\epsilon_{LF}-\epsilon_{HF}=38\,\epsilon_0\,,$$

$$\tau_{i0}=3\times10^{-16}\ \mathrm{s}\,,$$

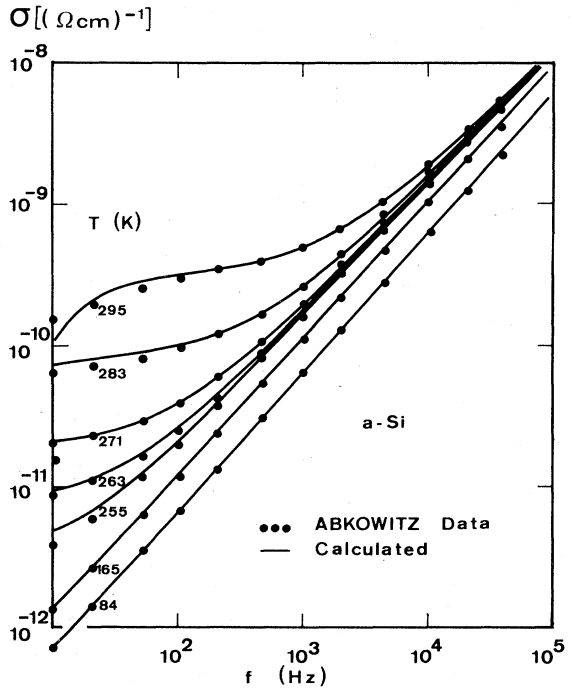

FIG. 14. (●) Experimental σ_{ac} data of Abkowitz in glow discharge *a*-Si. Solid lines: Conductivities calculated according to Eqs. (10) and (22).

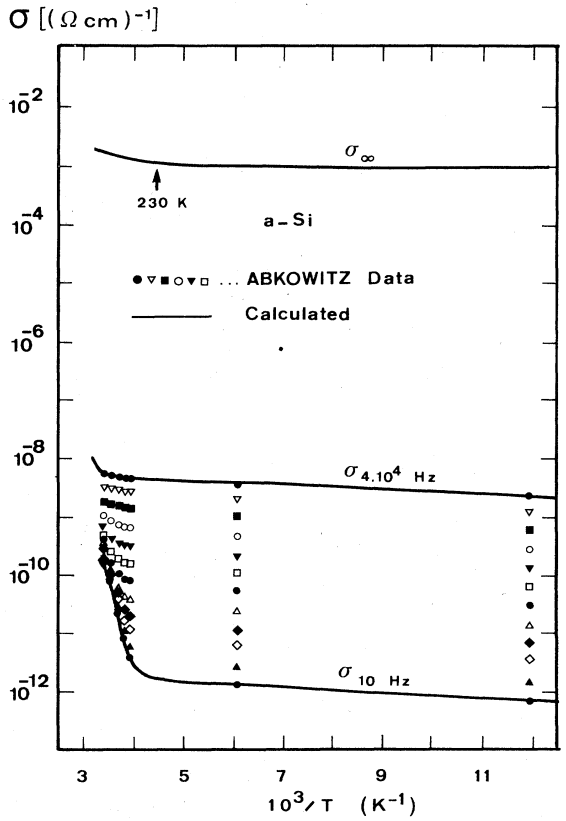

FIG. 15. (●▽■...) Experimental σ_{ac} data versus $10^3/T$ of Abkowitz for glow discharge *a*-Si. Solid lines: Conductivities calculated according to Eqs. (10), (14), and (22).

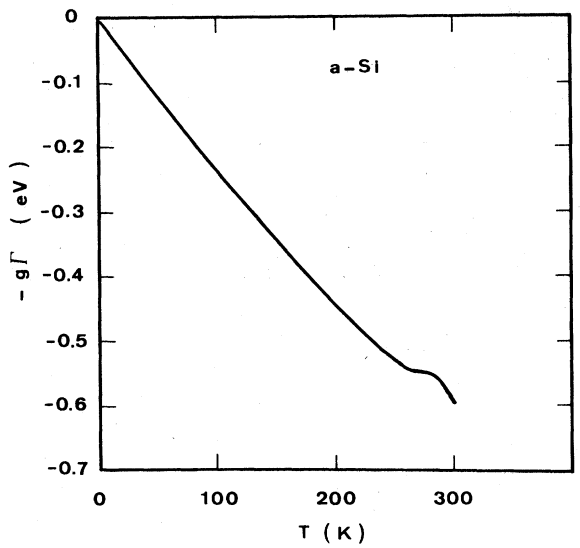

FIG. 16. $g\Gamma(T)$ corresponding to a-Si sample of Abkowitz.

$E_i = 0.796$ eV .

This level starts to ionize around 230 K, so that σ_∞ must increase above this temperature; the temperature dependence of σ_∞ shown in Fig. 15 is obtained by considering that E_F is staying at kT below the bottom of the wells and that μ_n remains constant. This variation of σ_∞ results in a slower variation of g with T, as previously anticipated; $g\Gamma$ is plotted versus T in Fig. 16. The fit of σ_{ac}, taking all these effects into account, is shown in Fig. 14. As observed, the agreement is very good at all frequencies and temperatures. The progressive ionization of the deep level as T increases is depicted by Fig. 17 where the abscissa is the probability $P(E_c)$ multiplied by α or $(1-\alpha)$. The fact that $s \simeq 1$ results from the large value of $g\Gamma/kT \simeq 30$ (see Fig. 2). In conclusion the consideration of band carriers and of large potential fluctuations leads to a complete and consistent explanation of the data.

B. Our data on P-doped a-Si:H

The films provided by Kaplan and co-workers at Thomson-CSF were deposited by chemical-vapor-deposition (CVD) on single-crystal silicon substrates held at 600 °C, from mixtures of pure silane, hydrogen, and phosphine in the gas phase.[15,16] The doping ratio $[PH_3]/[SiH_4]$ of the sample considered in this paper is 10^{-3}. Samples in sandwich configuration were obtained by evaporating (after etching) a titanium film 100-Å thick, covered by an Al electrode of 1000 Å.

Measurements of σ_{ac} and ϵ_{ac} were performed between 60 and 1000 Hz in the temperature range 4.2 to 24.5 K. The σ_{ac} data alone are correctly fitted by choosing the following values of the parameters: $\alpha = 0.09$, $\sigma_\infty = 8 \times 10^{-8}$ $(\Omega\,\text{cm})^{-1}$, $\Gamma = 20$ meV, g proportional to T, with $(g\Gamma/kT) = 18.2$ up to 32 K; above g remains constant. However, in order to fit both ϵ_{ac} and σ_{ac} plotted versus $\omega/2\pi$ in Fig. 18 it is necessary to add another contribution corresponding to $\alpha' = 0.12$, $\sigma'_\infty = 10^{-6}$ $(\Omega\,\text{cm})^{-1}$,

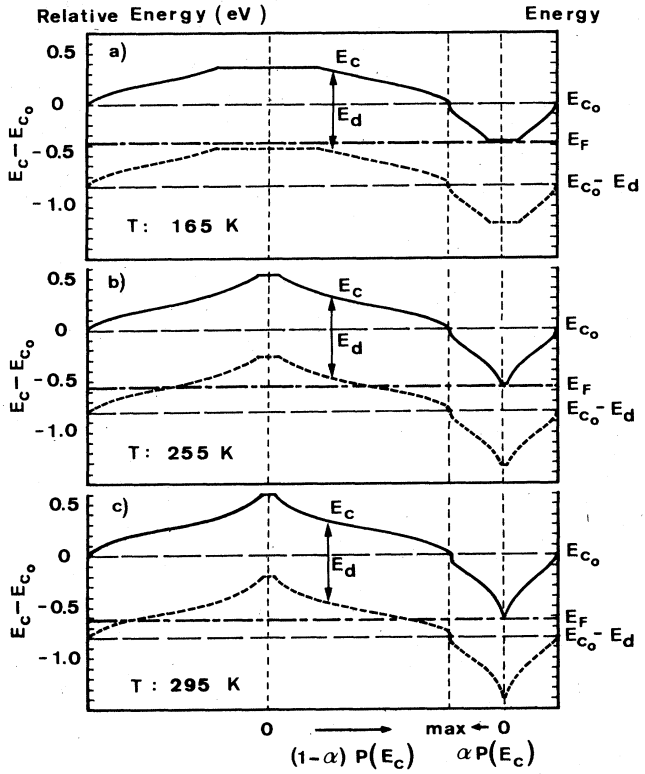

FIG. 17. Respective local positions of band edge, deep level ($E_d \equiv E_i = 0.796$ eV), and Fermi level in a-Si sample of Abkowitz at 165, 255, and 295 K, with probability as abscissa.

$\Gamma' = 15.6$ meV, and $g'\Gamma'/kT = 71$. This could be explained by some filamentary or columnar structure of the sample. However, the effect of the second contribution on σ_{ac} is very weak, so it is possible that the variation of ϵ_{ac} could also be accounted for by the charge and discharge of a deep center. The temperature dependence of the depth $g\Gamma$ of deepest wells is shown in Fig. 19; the position of the Fermi level obtained from Eq. (32) for $\mu_n = 3 \times 10^{-2}$ cm^2/V s, and $\mu_n = 1.5 \times 10^{-2}$ cm^2/V s is also plotted. It is interesting to note the low value of Γ (20 meV) found for this sample.

C. Data of Long and Balkan (Ref. 17) on a-Ge films obtained by thermal evaporation or RF sputtering

The conductance of the samples has been measured between 10 Hz and 100 KHz in the temperature range 1.3 to 102 K, as shown in Fig. 20. In order to evaluate the band conductivity we assume that the ratio of the area to the thickness of the sample is equal to 2×10^4 cm. The fit of the data is obtained by choosing $\alpha = 0.136$, $\sigma_\infty = 5 \times 10^{-7}$ $(\Omega\ \text{cm})^{-1}$, $\Gamma = 42.1$ meV, and $\Gamma g/kT = 18.6$ up to 68 K; above 68 K, g remains constant. The contribution of charge and discharge of a deep level is clear above 77 K. The characteristics of this level used in the fit are

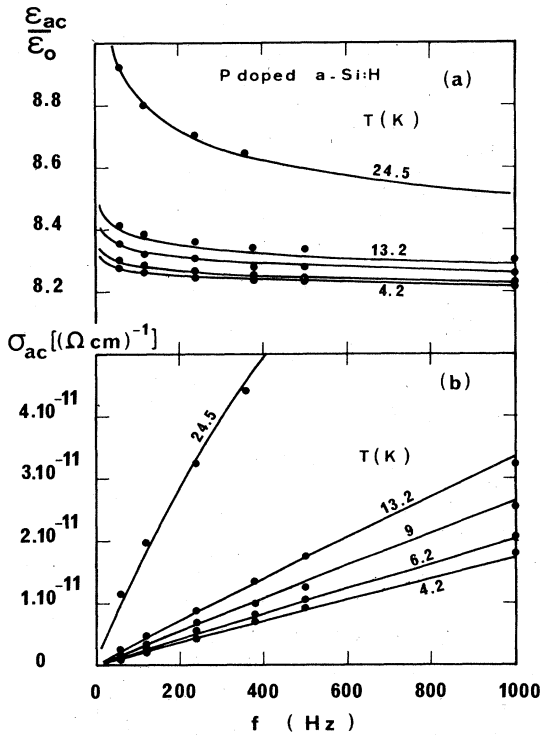

FIG. 18. (●) Our σ_{ac},ϵ_{ac} data on chemical-vapor-deposition P-doped *a*-Si:H. Solid lines: Calculated curves according to Eqs. (10) and (11). ϵ_{ac} tends to a limit $\epsilon_{sc}=8.03\,\epsilon_0$.

$$\epsilon_{LF}-\epsilon_{HF}=1.2\,\epsilon_0\ ,$$

$$\tau_{i0}=3.43\times10^{-7}\ \text{s}\ ,$$

$$E_i=51\ \text{meV}\ .$$

A second level which appears on the isotherms 77, 82.5, and 88.5 K has not been taken into account in the fit. No attempt to calculate the temperature dependence of σ_∞,

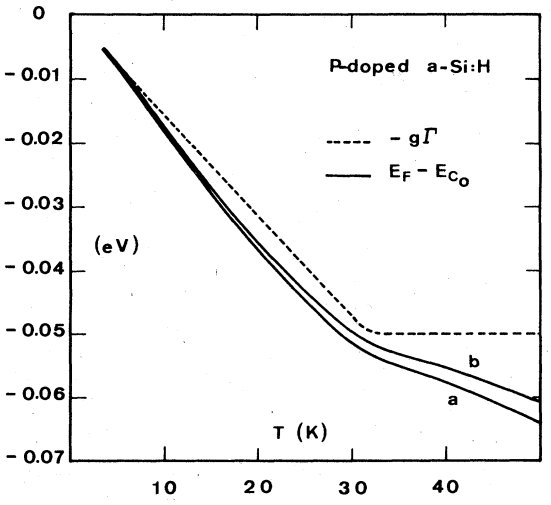

FIG. 19. Our *a*-Si:H sample. Dotted line: $g\Gamma$ versus T. E_F-E_{c0} (solid lines): (a) $\mu_n=3\times10^{-1}$ cm^2/V s; (b) $\mu_n=1.5\times10^{-1}$ cm^2/V s.

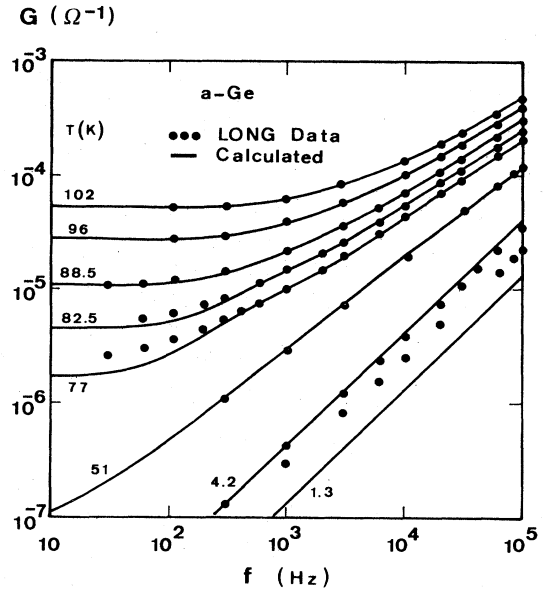

FIG. 20. (●) Experimental σ_{ac} data of Long on *a*-Ge. Solid lines: Calculated curves according to Eqs. (10) and (22).

when the ionization of this level is beginning, has been made. Using this constant value of σ_∞ we find $\mu_n=10^{-2}$ cm^2/V s, and this corresponds to a total carrier density in the band $n_0=3\times10^{14}$ cm^{-3}. Calculated curves are in quite good agreement with experiment at all temperatures from 4.2 to 102 K. At 1.3 K the calculated conductance is lower than the measured one.

In summary, the σ_{ac} data on various amorphous semiconductors obtained by different techniques may be well explained by considering only the conduction due to band carriers, the existence of potential fluctuations, and the presence of deep levels. Although some experimental data are lacking, the similarity of the phenomena with that observed in crystalline semiconductors likely results from similar conduction processes, and this is confirmed by the fact that the $g(T)$ dependence has exactly the expected behavior. Another interesting point is that the magnitude of potential fluctuations may greatly vary depending on the nature of the sample and the deposition process. The knowledge of Γ is certainly of prime importance in order to improve or compare manufacturing methods of amorphous films.

VIII. CONCLUSION

In compensated semiconductors potential fluctuations acting on band carriers result in a nonclassical frequency and temperature dependence of conductivity. The total carrier density in the band is fixed by an averaged neutrality equation which takes into account the fact that the average degree of ionization of deep centers is a function of the magnitude of fluctuations. This theory provides a self-consistent explanation of our data on semi-insulating GaAs, and of the ones reported by Pollak and Geballe on crystalline silicon; similar conclusions are proposed in the case of various amorphous semiconductors. In all these

samples, of quite different nature, the same general conduction process by band carriers in the presence of potential fluctuations is responsible for the observed conductivity. Contrary to a common opinion, it is unlikely that these data reflect the effect of hopping: This process is very likely hidden by the conduction due to high-mobility band carriers. It should be noted that the theory leads in all cases to a very accurate fit of the data, in very wide ranges of temperature and frequency including both dc and very high frequency. Such an agreement had not been previously approached by other models. In the case of amorphous semiconductors a better knowledge of σ_∞ and of the density of states in the gap would be desirable. If transport processes are involved in this determination, the effect of potential fluctuations must obviously be taken into account in order to reach the real density of states.

ACKNOWLEDGMENTS

We would like to express our gratitude to A. Mitonneau at Laboratoire d'Electronique et de Physique Appliquie, G. Poiblaud at Radio Technique Compelec who supplied semi-insulating crystals, and to D. Kaplan and A. Friederich at Thomson-CSF, and J. Baixeras at Laboratoire de Genie Electrique Paris, who kindly supplied amorphous samples.

[1]W. Shockley and J. Bardeen, Phys. Rev. **77**, 407 (1950).
[2]L. V. Keldysh and G. P. Proshko, Fiz. Tverd. Tela (Leningrad) **5**, 12 (1963) [Sov. Phys.—Solid State **5**, 12 (1964)].
[3]B. I. Shklovskii and A. L. Efros, Fiz. Tekh. Poluprovodn. **4**, 2 (1970) [Sov. Phys.—Semicond. **4**, 2 (1970)]; Zh. Eksp. Teor. Fiz. **60**, 867 (1971); **62**, 1156 (1972) [Sov. Phys.—JETP **33**, 468 (1971); **35**, 610 (1972).
[4]D. Redfield, Adv. Phys. **24**, 4 (1975); **24**, 463 (1975).
[5]H. Fritzsche, Solid State Commun. **9**, 1813 (1971).
[6]B. Pistoulet, J. L. Robert, J. M. Dusseau, and L. Ensuque, J. Non-Cryst. Solids **29**, 29 (1978).
[7]P. Girard, Doctorat d'Etat thesis, Montpellier, 1983; also B. Pistoulet, P. Girard, and G. Hamamdjian, J. Appl. Phys. **56**, 2268 (1984); **56**, 2275 (1984).
[8]M. Pollak and T. H. Geballe, Phys. Rev. **122**, 1742 (1961).
[9]S. Kirkpatrick, Phys. Rev. Lett. **27**, 1722 (1971); Rev. Mod. Phys. **45**, 4 (1973); **45**, 574 (1973).
[10]R. R. Senechal and J. Basinski, J. Appl. Phys. **39**, 3728 (1968).
[11]Y. Zohta, Solid-State Electron. **16**, 1029 (1973).
[12]G. M. Martin, J. P. Farges, G. Jacob, J. P. Hallais, and G. Poiblaud J. Appl. Phys. **51**, 5 (1980); **51**, 2840 (1980).
[13]Y. Yatsurugi, N. Akiyama, Y. Endo, and T. Nozaki, J. Electrochem. Soc. **120**, 975 (1973).
[14]M. Abkowitz, P. G. Le Comber, and W. E. Spear, Commun. Phys. **1**, 175 (1976).
[15]N. Sol, D. Kaplan, D. Dieumegard, and D. Dubreuil, J. Non-Cryst. Solids **35**, 291 (1980).
[16]J. Magarino, D. Kaplan, and A. Friederich, Philos. Mag. **45**, 3 285 (1982).
[17]A. R. Long and N. Balkan, J. Non-Cryst. Solids **35-36**, 415 (1980).